Thiol-Yne Chemistry of Diferrocenylacetylene. From Synthesis and Electrochemistry to Theoretical Studies

Sonia Bruña,[a, b,*] Antonio Valverde-González,[a, c] M. Merced Montero-Campillo,[d] Otilia Mó,[b, d] and Isabel Cuadrado[a, b]

[a]Departamento de Química Inorgánica, Facultad de Ciencias, Calle Francisco Tomás y Valiente, 7, Universidad Autónoma de Madrid, Ciudad Universitaria de Cantoblanco, 28049, Madrid, Spain.

[b]Institute for Advanced Research in Chemical Sciences (IAdChem), Facultad de Ciencias, Calle Francisco Tomás y Valiente, 7, Universidad Autónoma de Madrid, Ciudad Universitaria de Cantoblanco, 28049, Madrid, Spain.

[c]Present address: Sorbonne Université, CNRS, Institut Parisien de Chimie Moléculaire, Equipe Chimie des Polymères, 4 Place Jussieu, 75005 Paris, France

[d]Departamento de Química, Facultad de Ciencias, Calle Francisco Tomás y Valiente, 7, Universidad Autónoma de Madrid, Ciudad Universitaria de Cantoblanco, 28049, Madrid, Spain.

*email: sonia.brunna@uam.es

CONTENTS

1. Synthesis of diferrocenylacetylene (FcC≡CFc) 1.

In a 500 mL, three-necked flask, iodoferrocene **G** (2.21 g, 7.05 mmol) and copper(I) iodide H (1.46 g, 5.41 mmol) were added to 57 mL of distilled and purged pyridine, under argon. The resulting orange suspension was heated up to 125 °C for 3 hours. The dark-red solution was then poured into an ice bath, forming an orange and dense past. After filtering it with a sintered glass, the solid thus obtained was repetitively washed with water until neutrality, and finally with hot toluene. The reddish organic phase was dried over anhydrous $MgSO_4$ and was finally purified by column chromatography on silica gel (10 cm x 2 cm). With *n*-hexane the unreacted **G** was eluted, while the desired diferrocenylacetylene **1** was obtained on eluting with toluene. Yield: 1.71 g (80%). ^{1}H NMR ($CDCl_3$, 300 MHz): δ4.20, 4.45 (pt, 8H, C_5H_4), 4.23 (s, 10H, C_5H_5). ^{13}C NMR ($CDCl_3$, 75 MHz): δ66.4 (*ipso*-Fc), 68.6, 71.3 (C_5H_4), 70.1 (C_5H_5), 84.1 (*C*≡*C*). IR (KBr, cm^{-1}): ν(C–H) 3099, ν(C=C) 1261, δ(C–H) 805, δ(Fe–Cp) 481. MS (MALDI-TOF): *m/z* 394.0 [M$^+$].

2. Characterization of starting materials and compounds 2 and 3

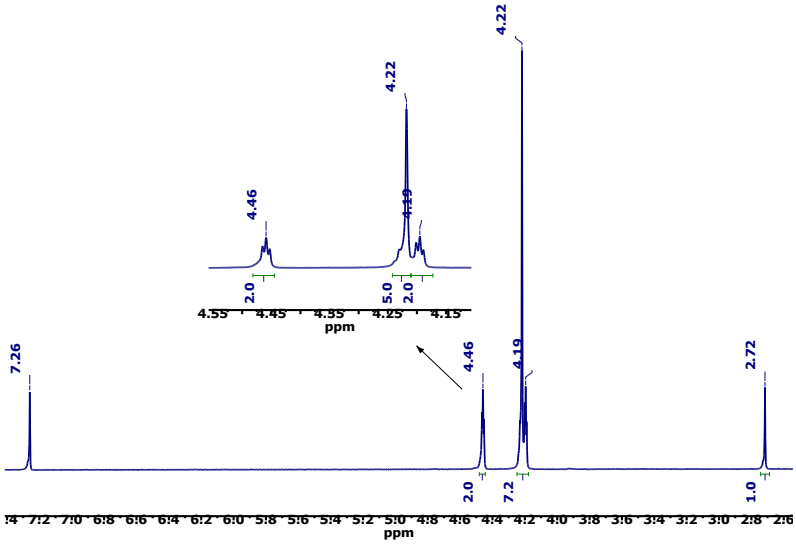

Figure S1: ^{1}H NMR spectrum of ethynylferrocene **B** (300 MHz, $CDCl_3$).

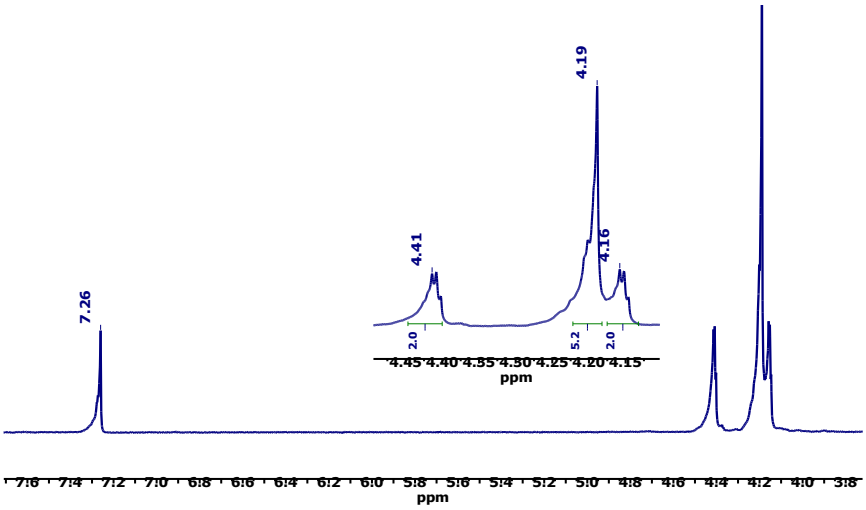

Figure S2: ^{1}H NMR spectrum of iodoferrocene **G** (300 MHz, $CDCl_3$).

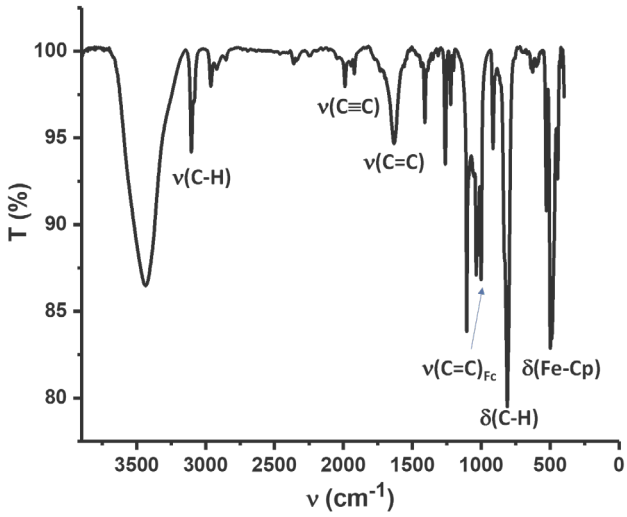

Figure S3: IR of cuprous ferrocenylacetylide **H**.

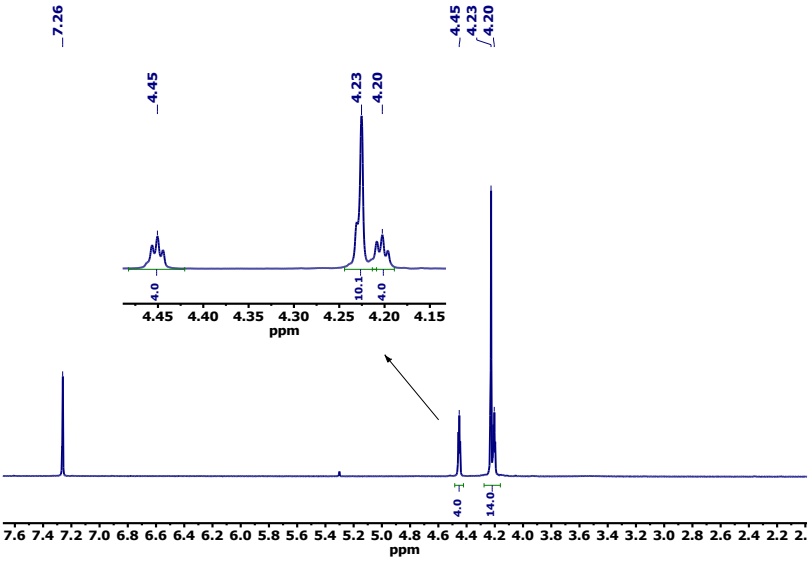

Figure S4: ^{1}H NMR spectrum of diferrocenylacetylene **1** (300 MHz, $CDCl_3$).

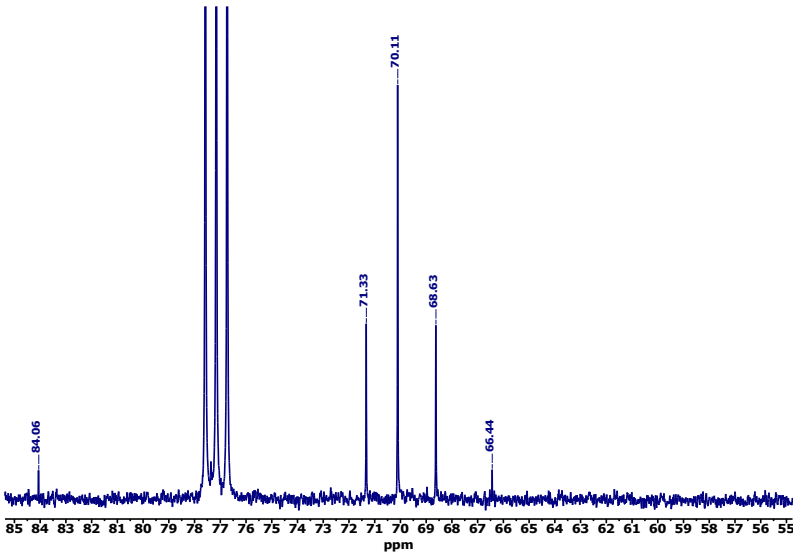

Figure S5: ^{13}C{^{1}H} NMR spectrum of diferrocenylacetylene **1** (75 MHz, $CDCl_3$).

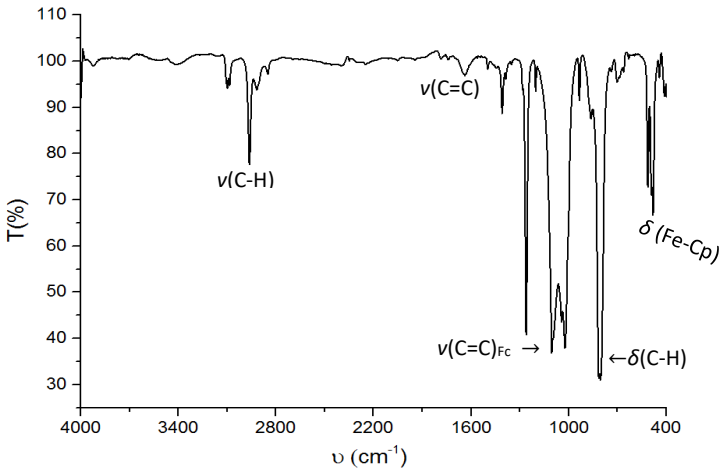

Figure S6: IR spectrum (KBr) of diferrocenylacetylene **1**

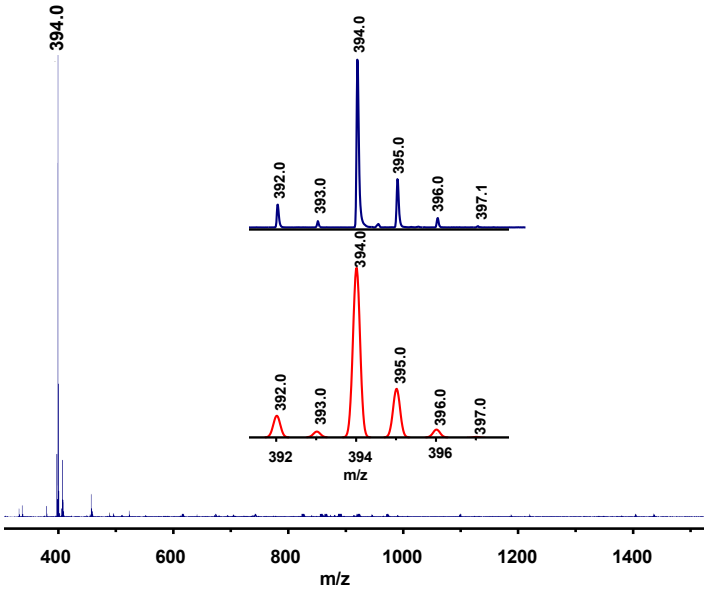

Figure S7: MALDI-TOF mass spectrometry of diferrocenylacetylene **1.**
Inset: isotopic distribution of molecular ion peak (top: experimental; bottom: calculated).

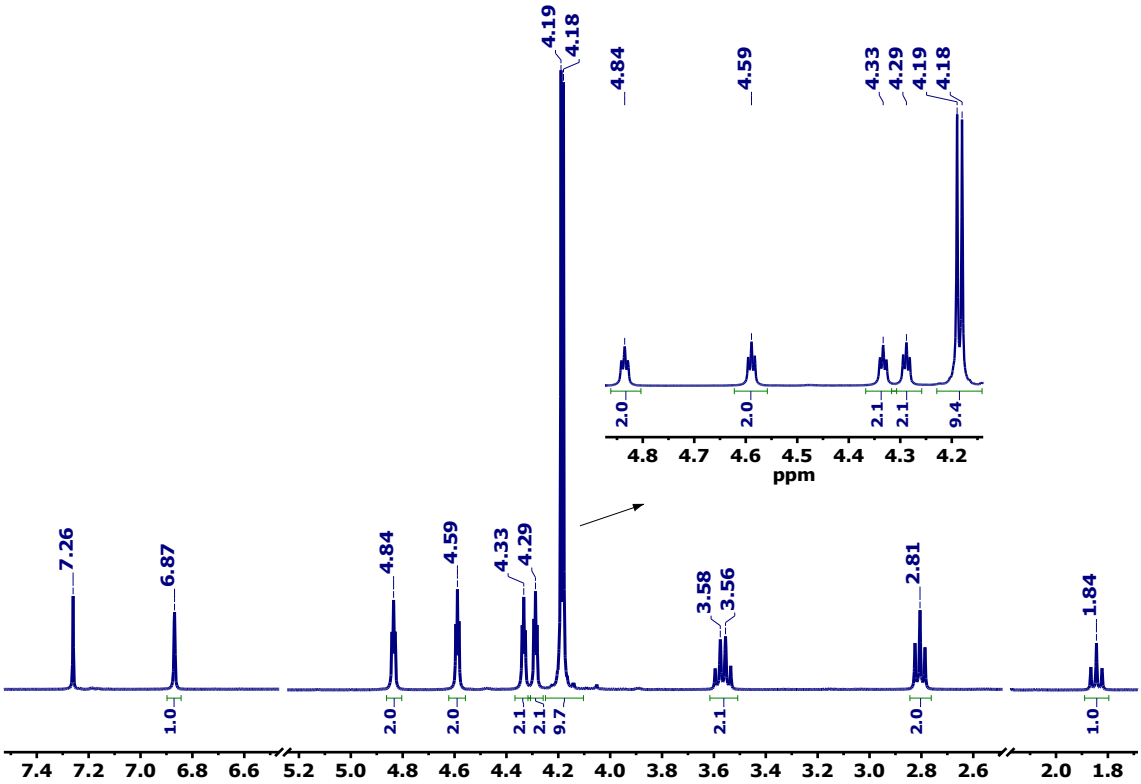

Figure S8: ^{1}H NMR spectrum of (*Z*)–stereoisomer FcCH=C(Fc)S–$(CH_2)_2OH$ (**2*Z***) (300 MHz, $CDCl_3$).

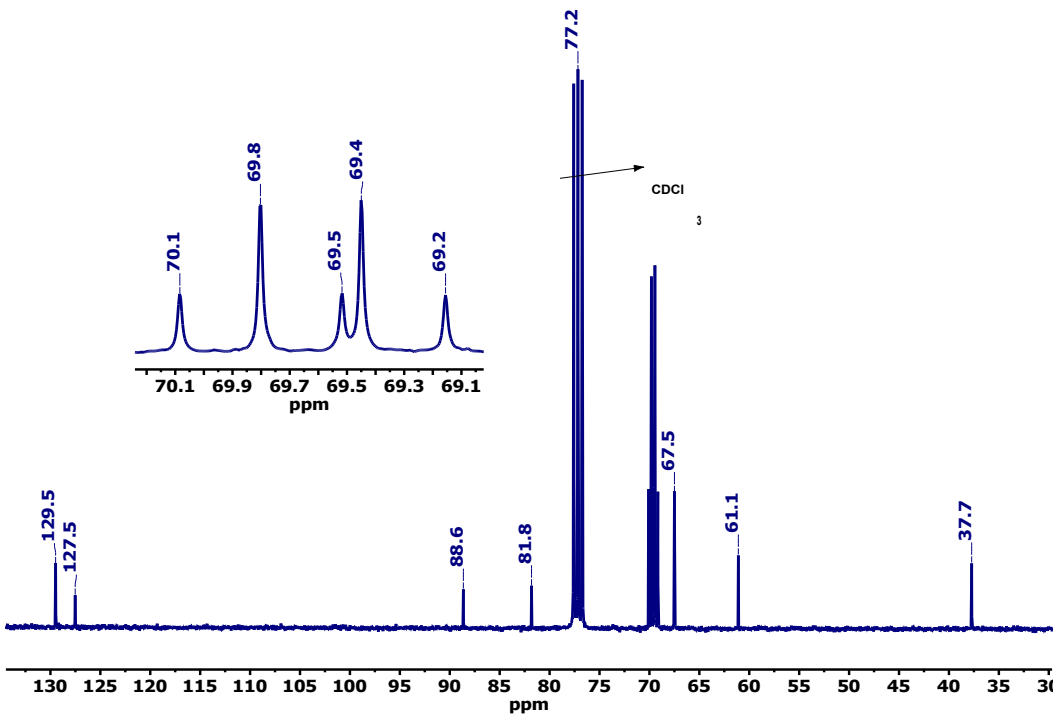

Figure S9: $^{13}C\{^{1}H\}$ NMR spectrum of (*Z*)–stereoisomer FcCH=C(Fc)S–$(CH_2)_2OH$ (**2*Z***) (75 MHz, $CDCl_3$).

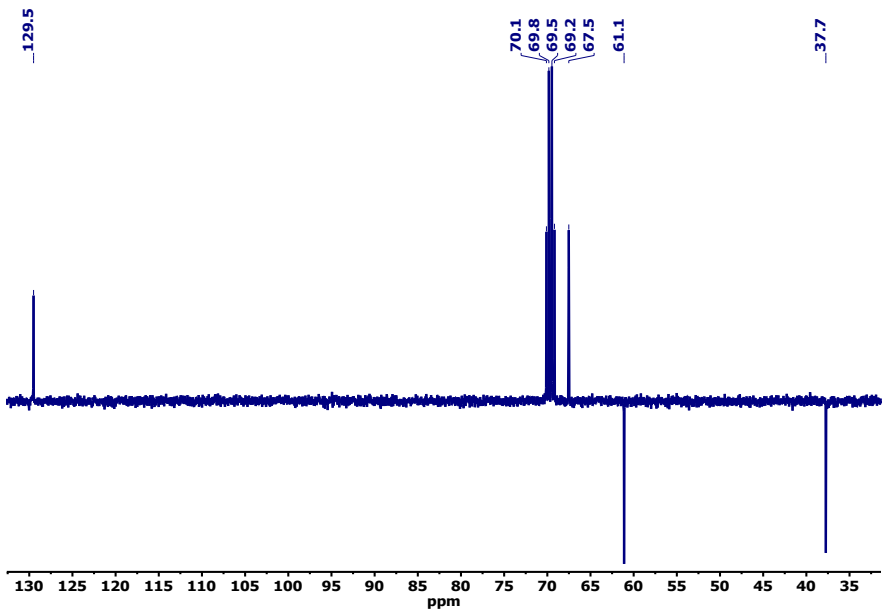

Figure S10: ^{13}C-NMR DEPT-135 of (*Z*)–stereoisomer FcCH=C(Fc)S–$(CH_2)_2OH$ (**2*Z***) (75 MHz, $CDCl_3$).

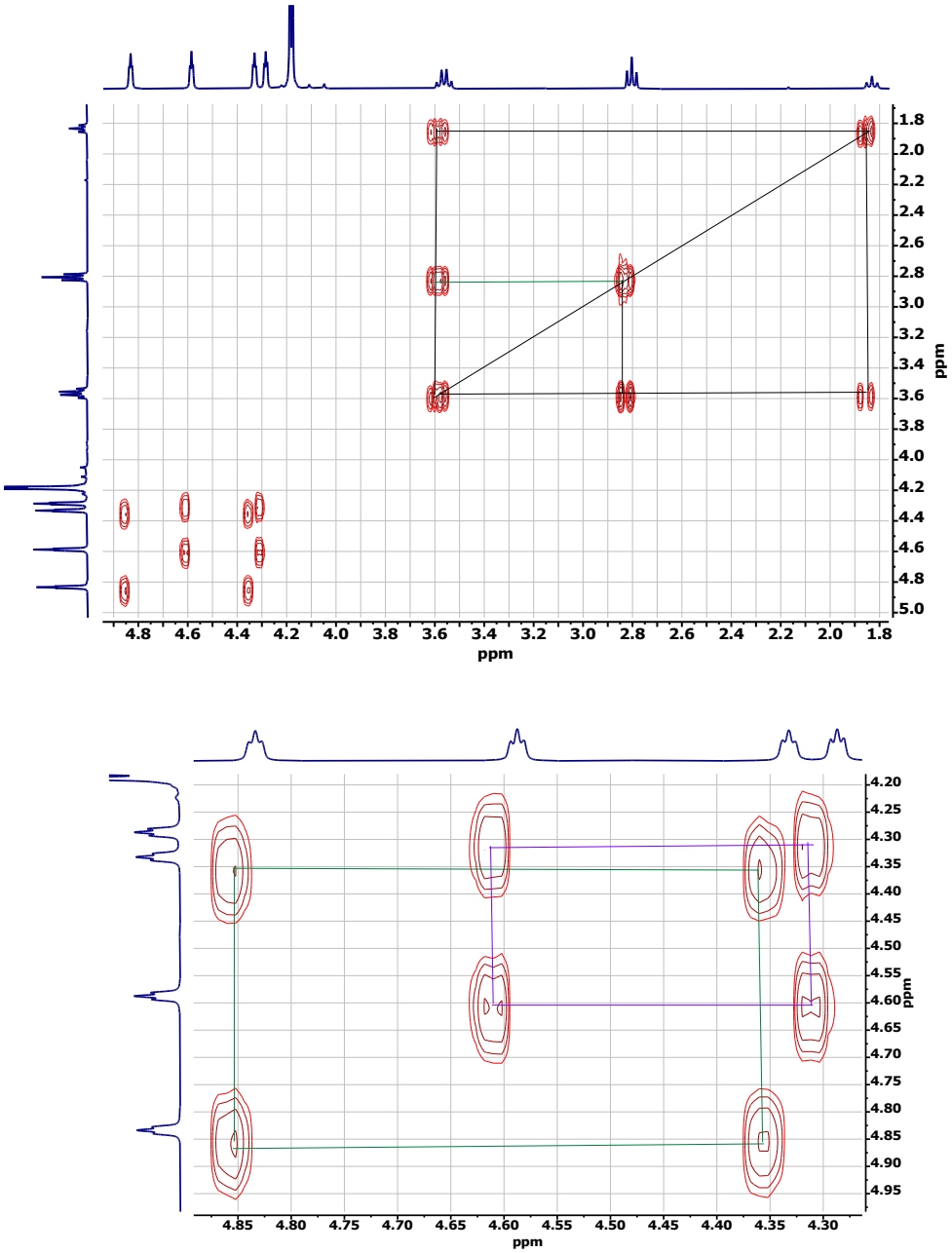

Figure S11: Top: ^{1}H-^{1}H COSY NMR spectrum of (*Z*)–stereoisomer FcCH=C(Fc)S–$(CH_2)_2OH$ (**2*Z***) (300 MHz, $CDCl_3$). **Bottom:** expanded view of the ferrocenyl region.

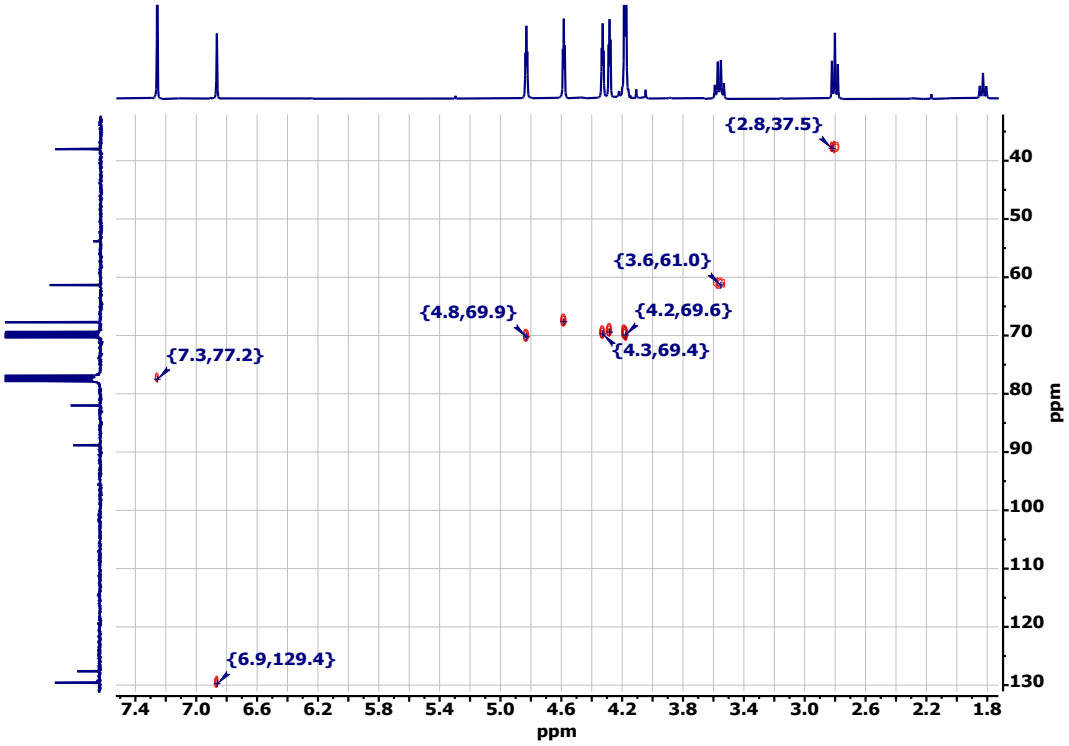

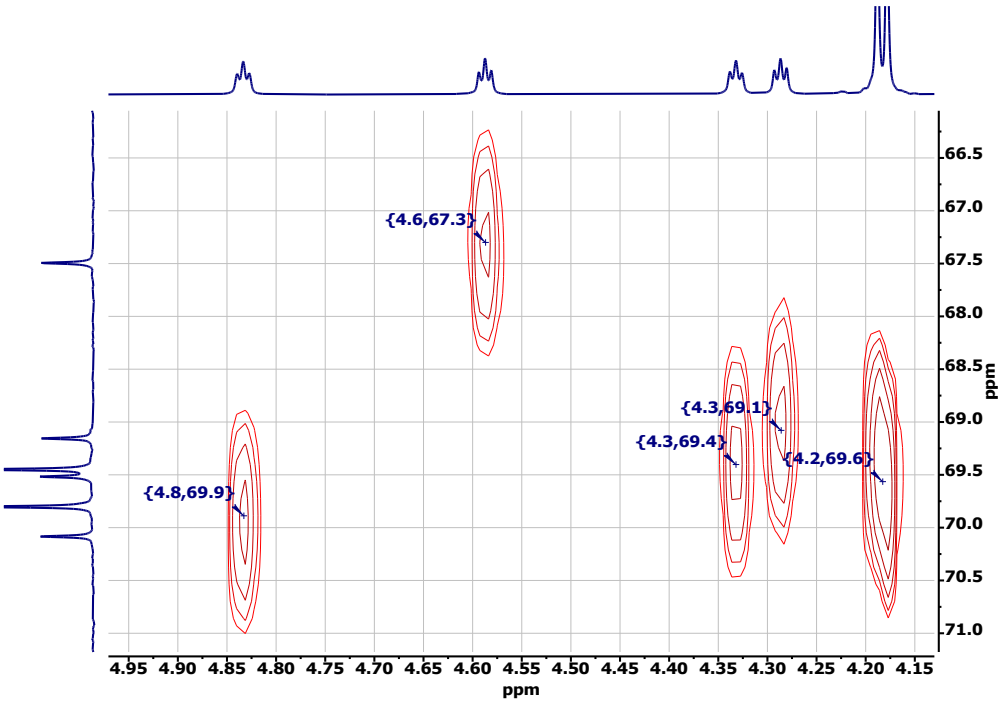

Figure S12: Top: ^{1}H–^{13}C HMQC spectrum of (*Z*)–stereoisomer FcCH=C(Fc)S–$(CH_2)_2OH$ (**2*Z***) (300 MHz, 75 MHz, $CDCl_3$). **Bottom:** expanded view of the ferrocenyl region.

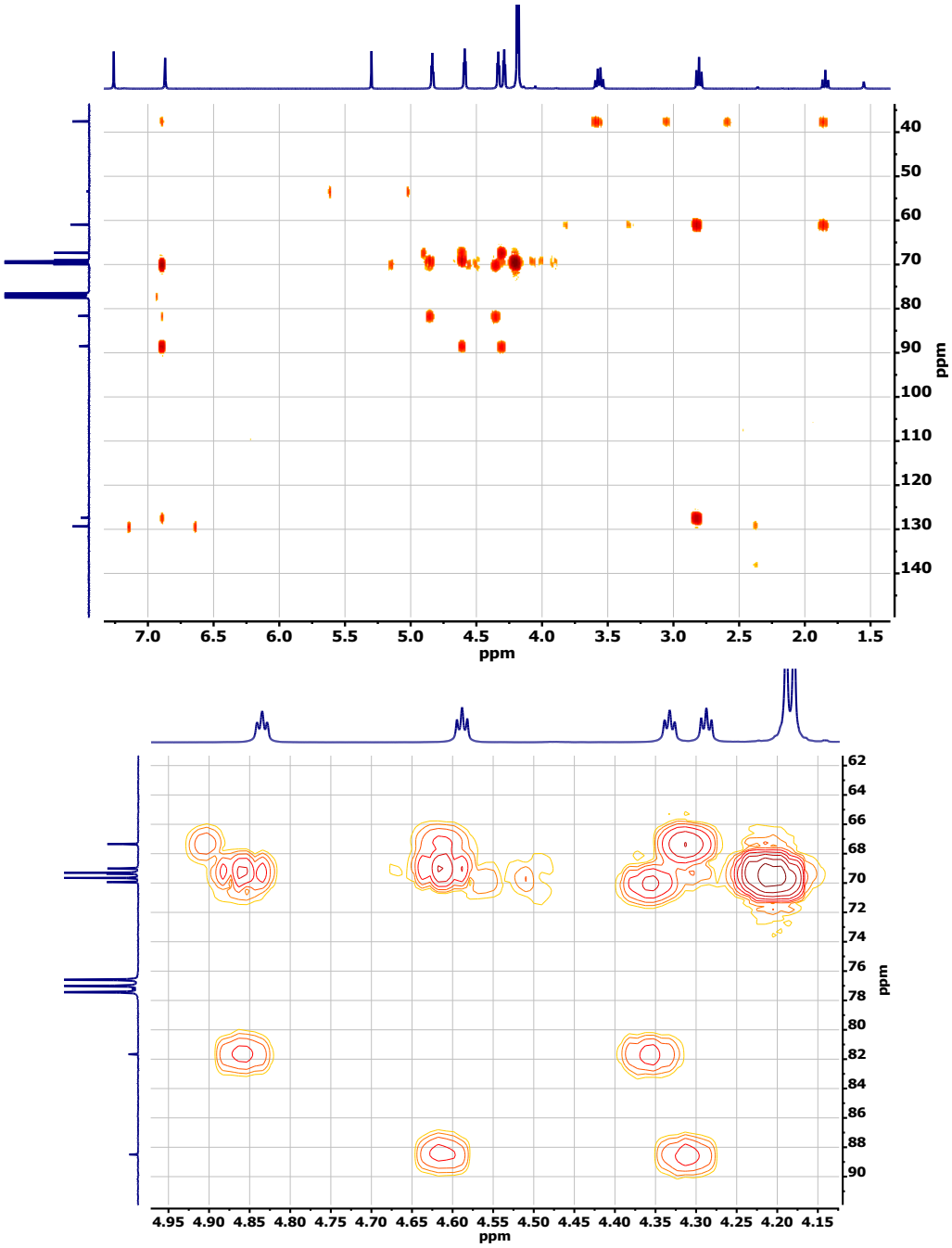

Figure S13: Top: ^{1}H–^{13}C HMBC spectrum of (*Z*)–stereoisomer FcCH=C(Fc)S–$(CH_2)_2OH$ (**2*Z***) (300 MHz, 75 MHz, $CDCl_3$). **Bottom:** expanded view of the ferrocenyl region.

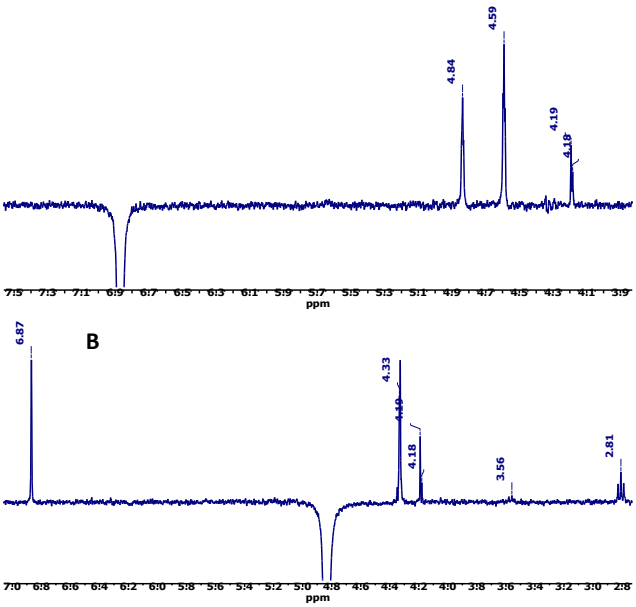

Figure S14: ^{1}H selective 1D NOE spectra of (*Z*)–stereoisomer FcCH=C(Fc)S–$(CH_2)_2$OH (**2*Z***) (300 MHz, $CDCl_3$), selectively irradiated at 6.87 ppm (A) and 4.84 ppm (B).

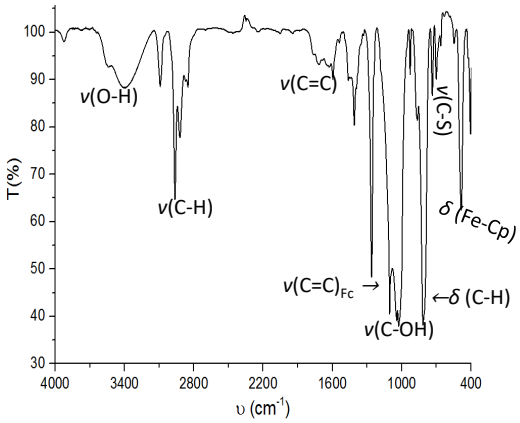

Figure S15: IR spectrum (KBr) of (*Z*)–stereoisomer FcCH=C(Fc)S–$(CH_2)_2$OH (**2*Z***).

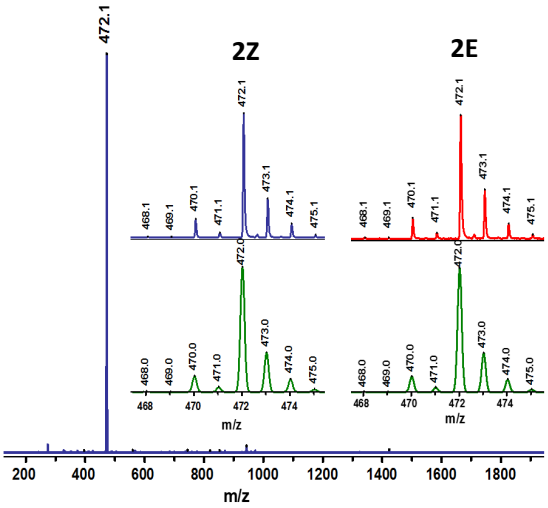

Figure S16: MALDI-TOF mass spectrometry of (*Z*)–stereoisomer FcCH=C(Fc)S–$(CH_2)_2$OH (**2*Z***). Inset: isotopic distribution of molecular ion peaks for **2*Z*** and **2*E*** (top: experimental; bottom: calculated).

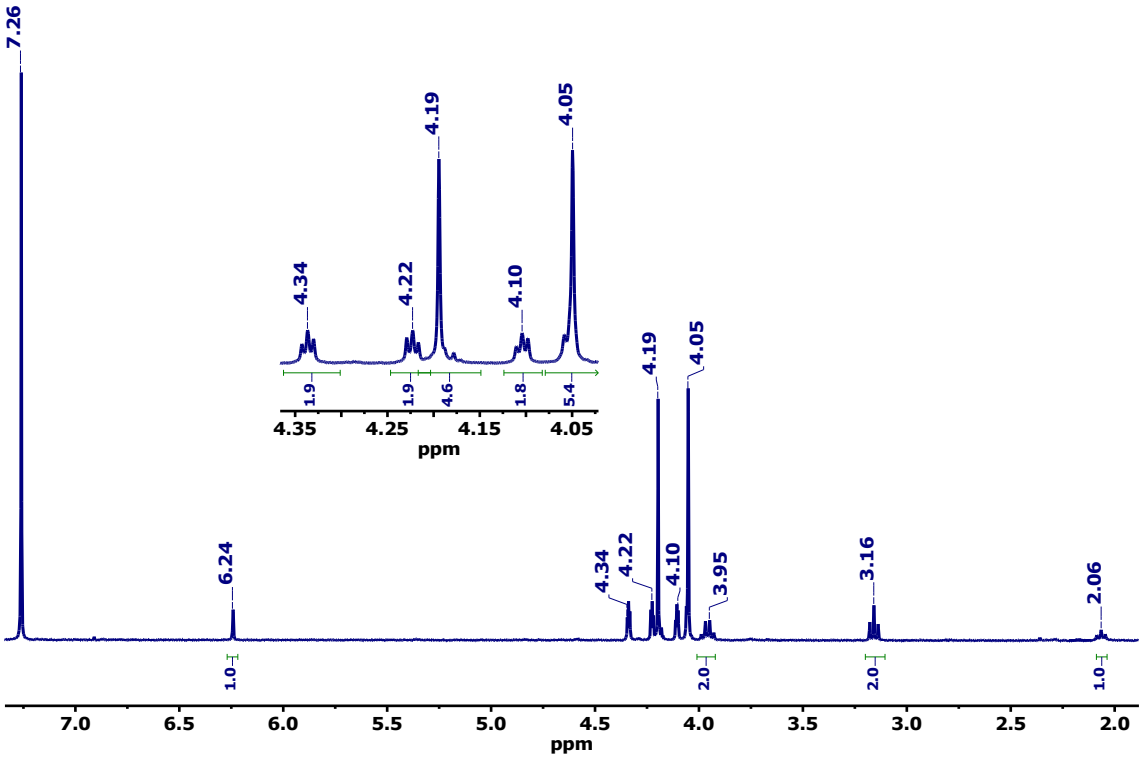

Figure S17: ^{1}H NMR spectrum of (*E*)–stereoisomer FcCH=C(Fc)S–$(CH_2)_2$OH (**2*E***) (300 MHz, $CDCl_3$).

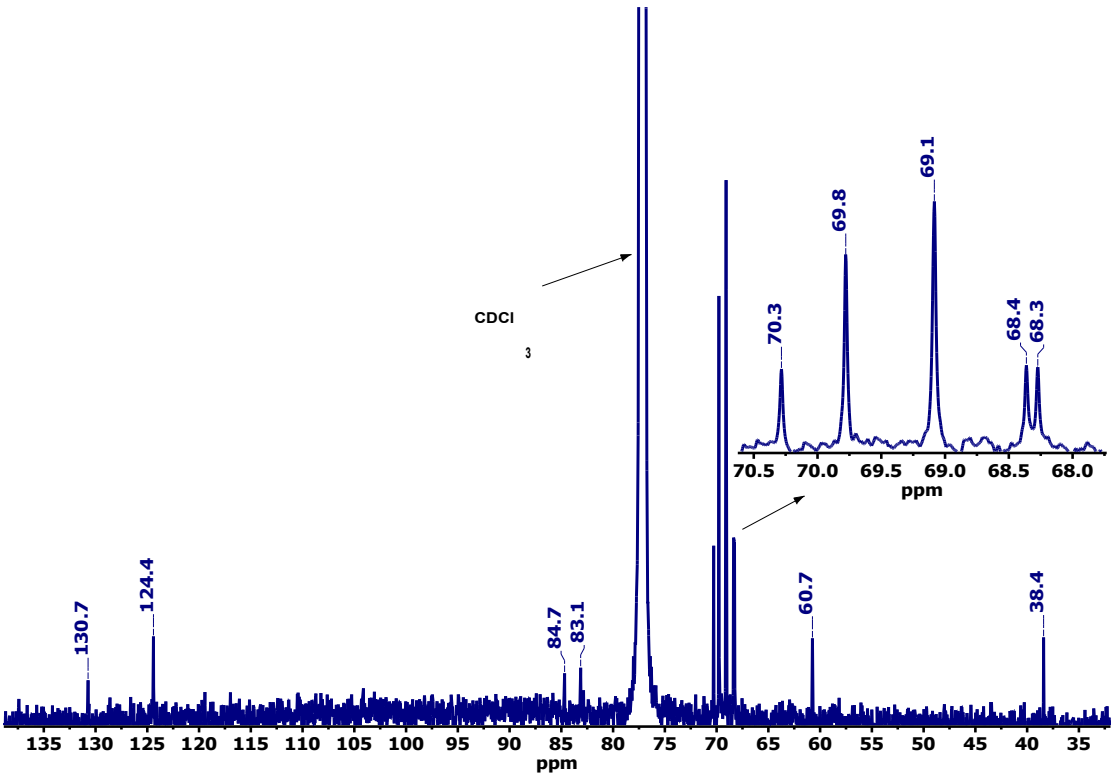

Figure S18: ^{13}C{^{1}H} NMR spectrum of (*E*)–stereoisomer FcCH=C(Fc)S–$(CH_2)_2$OH (**2*E***) (75 MHz, $CDCl_3$).

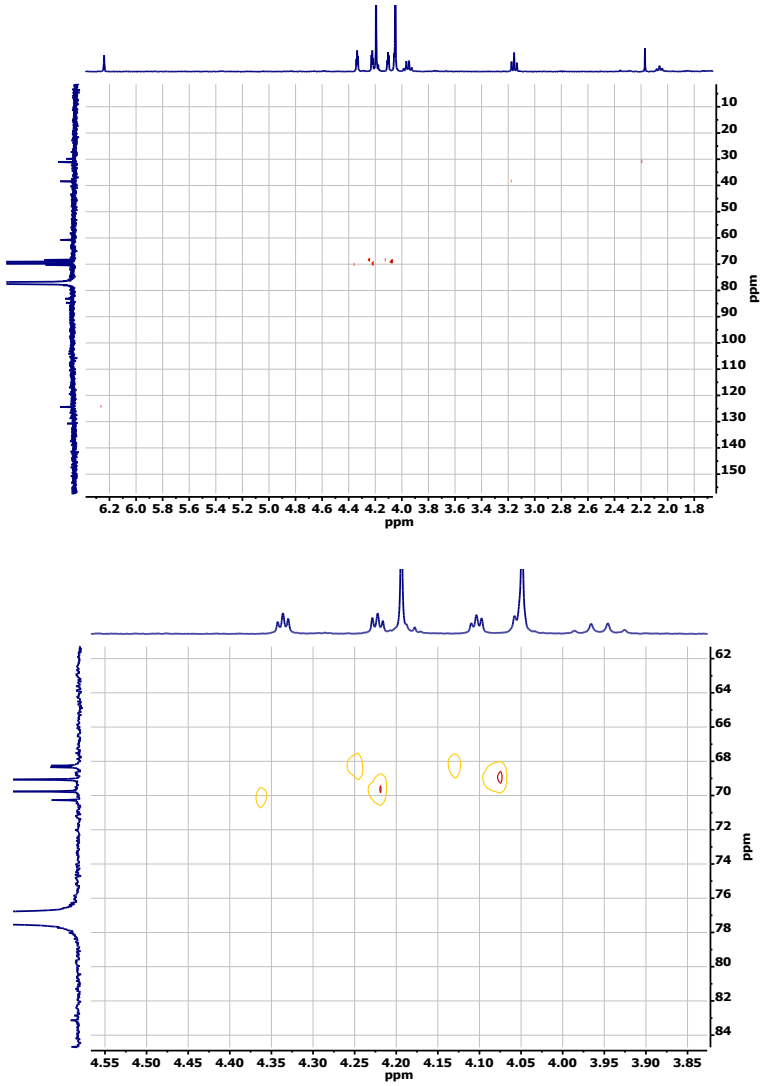

Figure S19: Top: ^{1}H–^{13}C HMBC spectrum of *E*)–stereoisomer FcCH=C(Fc)S–$(CH_2)_2OH$ (**2*E***) (300 MHz, 75 MHz, $CDCl_3$). **Bottom:** expanded view of the ferrocenyl region.

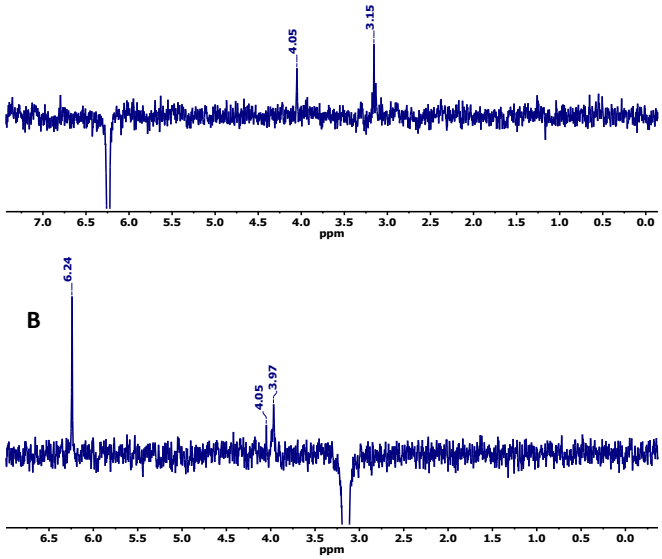

Figure S20: ^{1}H selective 1D NOE spectra of (*E*)–stereoisomer FcCH=C(Fc)S–$(CH_2)_2OH$ (**2*E***) (300 MHz, $CDCl_3$), selectively irradiated at 6.24 ppm (A) and 3.15 ppm (B).

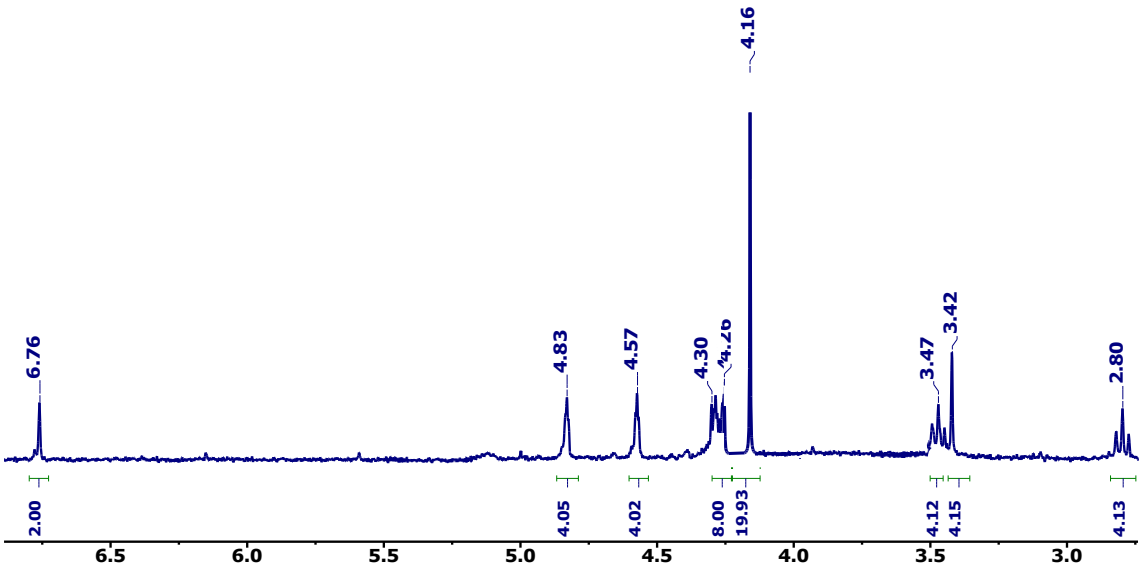

Figure S21: ^{1}H NMR spectrum of tetraferrocenyl– thioether stereoisomer **3*ZZ*** (300 MHz, $CDCl_3$).

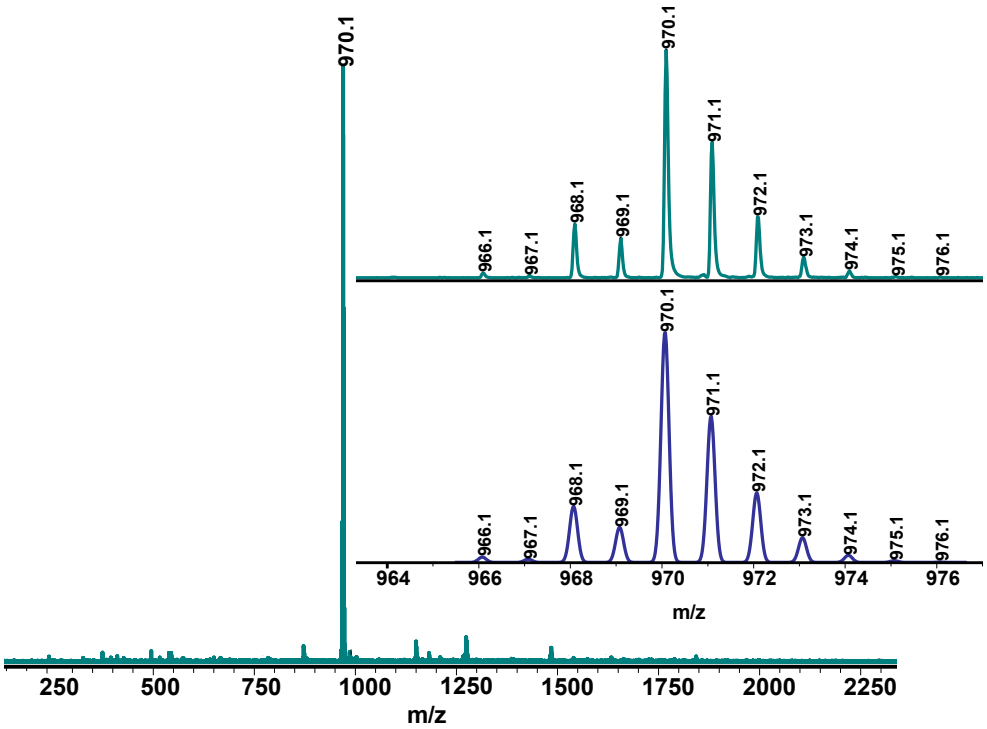

Figure S22: MALDI-TOF mass spectrometry of tetraferrocenyl– thioether stereoisomer **3*ZZ***. Inset: isotopic distribution of the molecular ion peak (top: experimental; bottom: calculated).

3. Theoretical studies

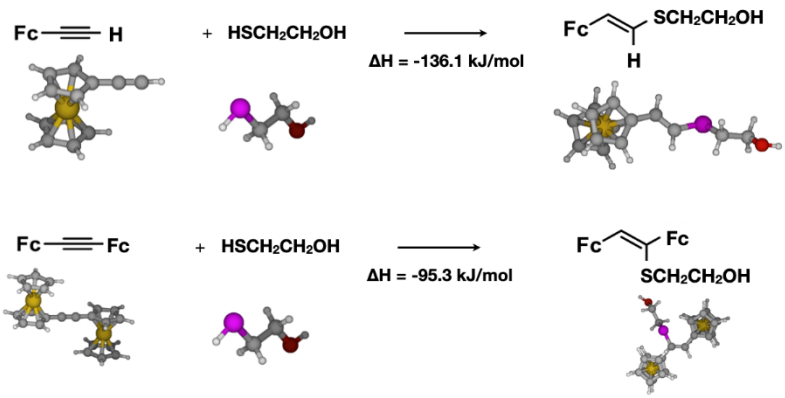

Figure S23. Optimized structures at the B3LYP/6-31+G(d) level of theory and total enthalpy reaction values for the first thiol addition to ethynylferrocene **B** and diferrocenylacetylene **1**. Both additions are largely exothermic in vacuum.

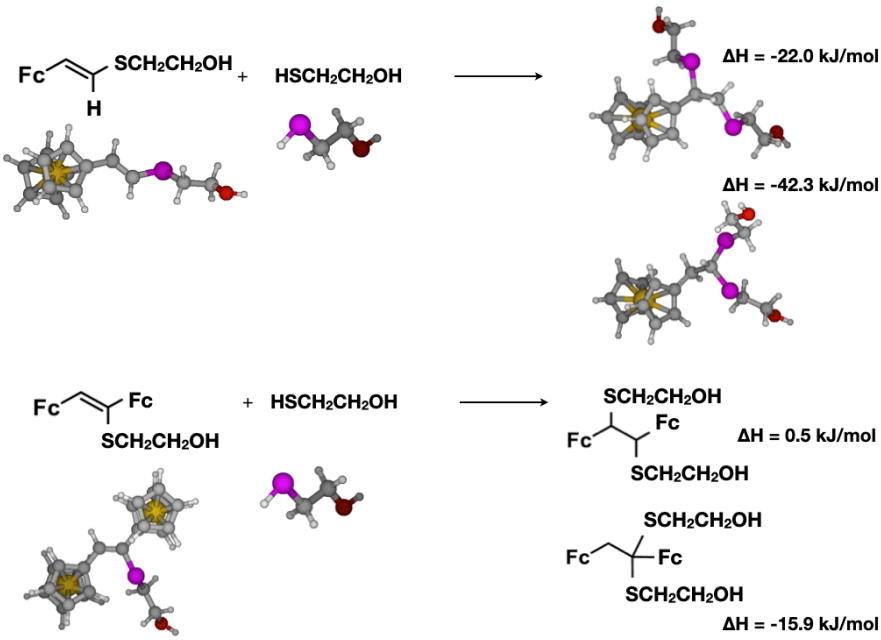

Figure S24. Optimized structures at the B3LYP/6-31+G(d) level of theory and total enthalpy reaction values for the second thiol addition to ferrocenyl vinyl sulfide and diferrocenyl vinyl sulfide. This step is significantly less exothermic for diferrocenyl vinyl sulfide or even not favored depending on the final product.

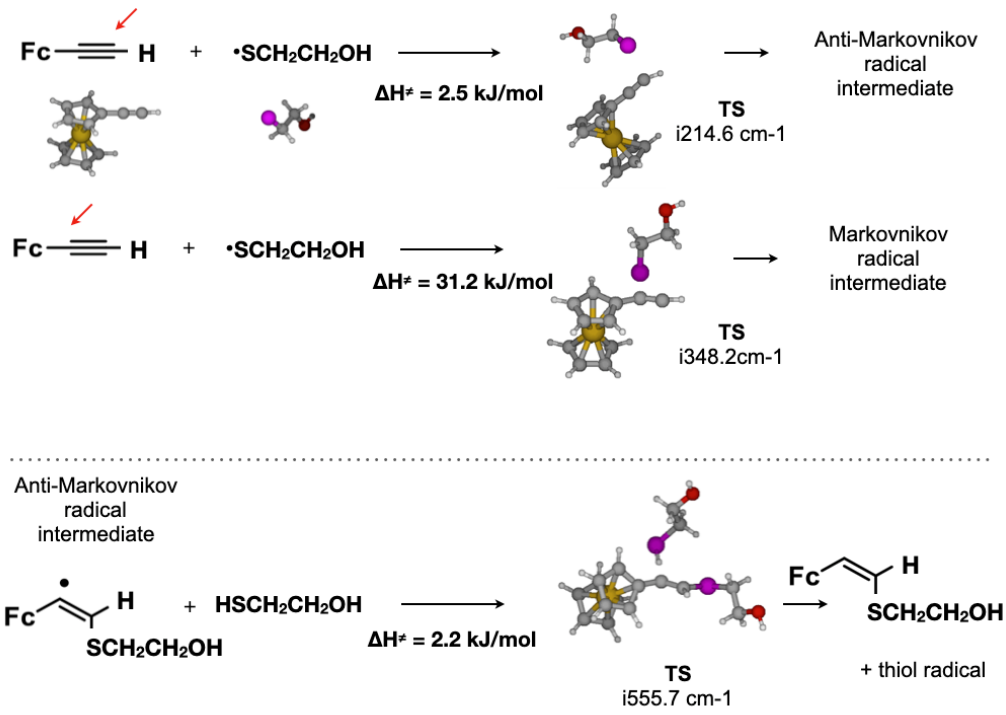

Figure S25. Optimized structures for transition states at the B3LYP/6-31+G(d) level of theory along with their relative enthalpic values with respect to the reactants for the first thiol addition to ethynylferrocene **B**.

The thiol addition to ethynylferrocene is anti-Markovnikov because the barrier to interact with the external carbon is significantly lower than the one found for the internal carbon (2.5 vs 31.2 kJ·mol^{-1}). The following step is also almost barrierless (2.2 kJ·mol^{-1}). The nature of the two carbon atoms of the alkyne reagent is in fact quite different. The atomic charges assigned by the NBO (Natural Bond Order) method indicate that the terminal carbon is much charged than the internal one (-0.230 vs -0.009). We could not locate at the same level of theory similar transition states for diferrocenylacetylene **1**, what might have several explanations. Considering the symmetric nature of the alkyne, none of the two carbons should be favored to react with the thiol radical, and the steric hindrance would be pretty similar for the same reason.

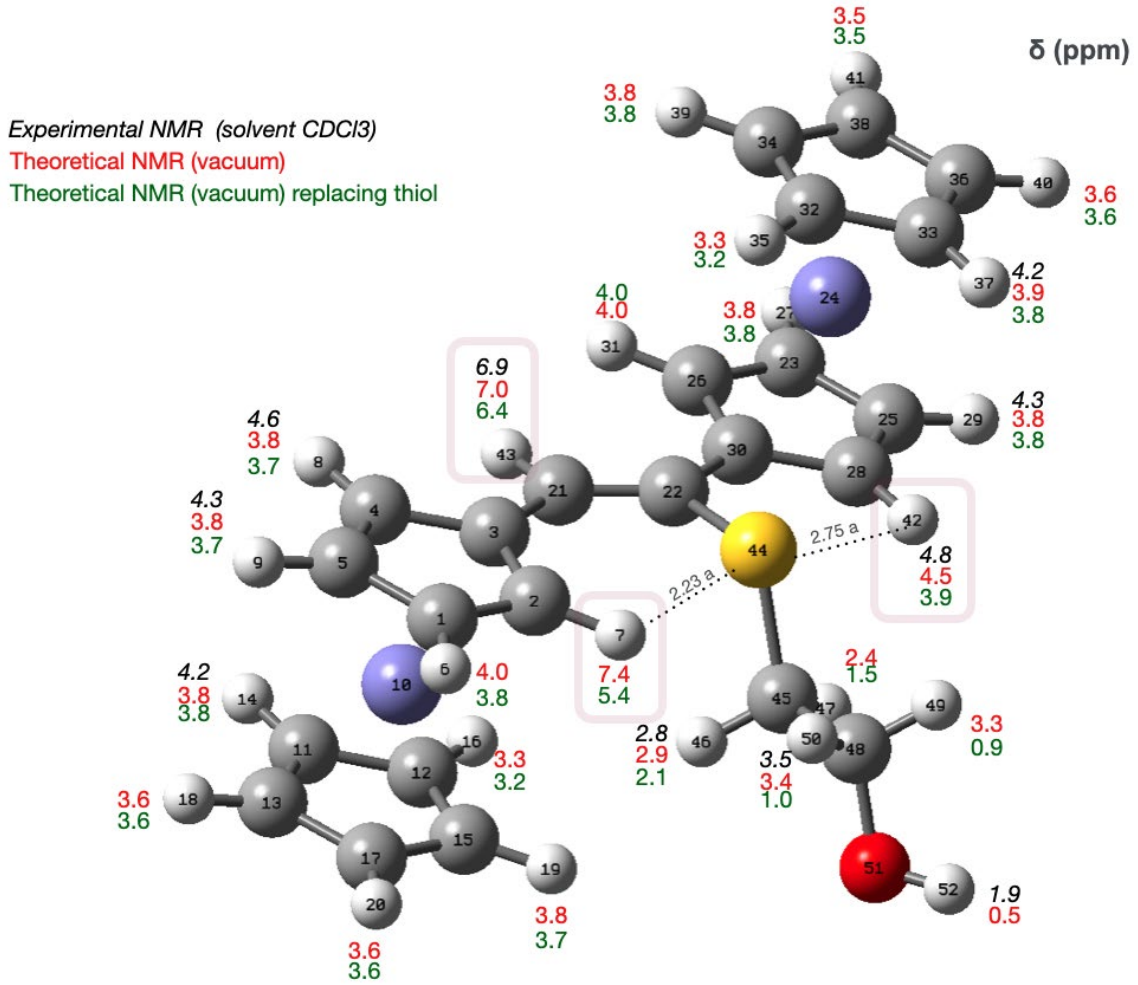

Figure S26. NMR theoretical results carried out at the B3LYP/6-311++G(d,p) level of theory for the **2*Z*** isomer.

NMR theoretical results are shown in the picture for the pure **2*Z*** isomer in its equilibrium structure. Black values stand for the experimental NMR results in solution, whereas the red values are those obtained in vacuum at the B3LYP/6-311++G(d,p)//B3LYP/6-31+G(d) level of theory with respect to the standard TMS reference with the GIAO method. Additionally, we included the results obtained when the full thiol chain is replaced by a propyl chain, in order to see the effect of the thiol substituent. A first look evidences that the experimental and theoretical values are fully consistent along the whole structure, taking into account the physicochemical differences underlying both series of results (geometries and surrounding environment). As can be noticed looking at the red numbers, the hydrogen atom from the vinyl unit is significantly shifted (7.0 ppm) with respect to the analogous propyl-substituted derivative (6.4 ppm), and in good agreement with the experimental value (6.84 ppm). The sulfur atom is responsible for the largest theoretical shift observed (7.4 ppm), because of the short distance in the equilibrium geometry between H and S. Instead, a H atom located at a much larger distance presents a value of 4.5 ppm, in line with the experimental result (4.8 ppm). It is important to note that the experimental result is an average of the H atom values that, because of rotation, may interact with sulfur. It is interesting also to compare the different values for the hydrogens of the Cp rings, showing larger deshieldings for the Cp units bonded to the alkene moeity, and the null effect of the thiol chain on distant hydrogens.

Compound	C-C triple bond dist (Å)	Dipolar moment (D)
HCCH	1.208	0.0000
FCCF	1.193	0.0000
LiCCLi	1.256	0.0000
FcCCH	1.212	0.9850
FcCCFc (**1**)	1.217	0.0001
PhCCPh	1.217	0.0004

Table S1. Triple C-C bond distances (Å) obtained in vacuum at the B3LYP/6-31+G* level of theory for the optimized structures of diferrocenyl acetylene **1** and some related compounds, along with their dipolar moment (D).

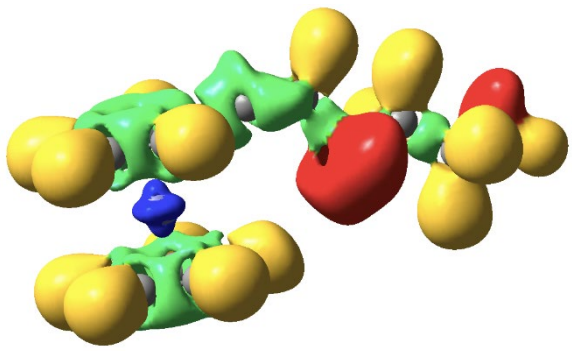

Figure S27. ELF function (ELF = 0.70) for the alkene radical derived from **B**. Green lobes are polysynaptic basins, whereas red lobes correspond to lone pairs, blue to the iron core and yellow to disynaptic basins involving hydrogens. At this ELF value, it is possible to clearly locate a green bump associated to the unpaired electron over the C directly attached to the ferrocenyl unit.

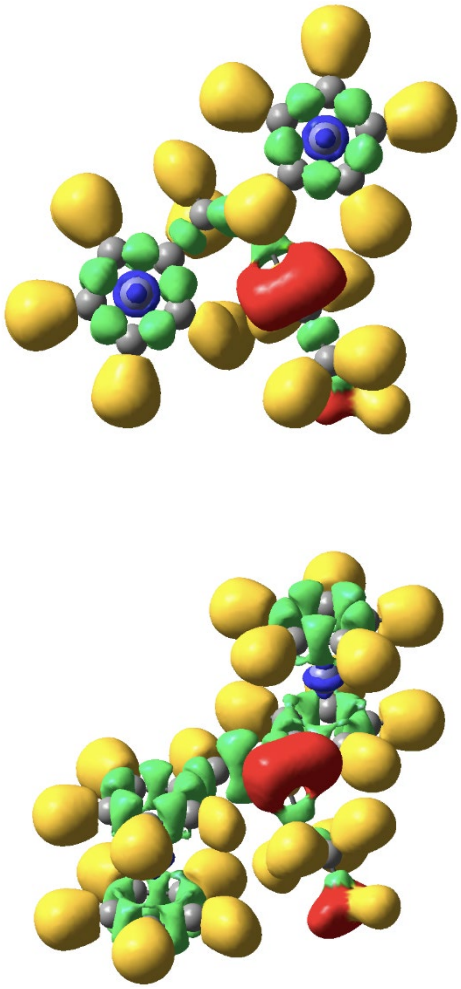

Figure S28. Two views of the ELF function (ELF = 0.70) for the neutral alkene **2Z**. Green lobes are polysynaptic basins, whereas red lobes correspond to lone pairs, blue to the iron core and yellow to disynaptic basins involving hydrogens. See population analysis below the picture, where Fe(1) corresponds to the Fc moiety attached to (CH) and Fe(2) corresponds to the Fc moiety attached to (CSR).

Neutral **2*Z*** isomer

Core Fe(1) 24.12 e-
Sum basins (Fe1, C(Cp) linked to alkene) 1.87 e-
Sum basins (Fe1, C(Cp)) 1.86 e-
Core Fe(2) 23.85 e-
Sum basins (Fe1, C(Cp) linked to alkene) 2.03 e-
Sum basins (Fe1, C(Cp)) 1.94 e-

Cation of **2*Z*** isomer

Core Fe(1) 24.13 e-
Sum basins (Fe1, C(Cp) linked to alkene) 1.82 e-
Sum basins (Fe1, C(Cp)) 1.75 e-

Core Fe(2) 23.70 e-
Sum basins (Fe1, C(Cp) linked to alkene) 1.86 e-
Sum basins (Fe1, C(Cp)) 1.38 e-

The ELF shows the ferrocenyl units as Fe^{2+} cores (around 24 electrons) surrounded by 10 Fe-C(Cp) basins. These Fe-C(Cp) basins are located between the core and the ring planes. Each of these iron-carbon basins is populated by approx. 0.4e-, i.e., for each Fe^{2+}:Cp interaction there are mostly 0.4e- x 5 = 2e-. This is in line with a view of ferrocene as a system arising from neutral iron core giving 2e- to bind with the 2e- donated by the 2 Cp units. All in all, in the neutral system we should have in the sandwich region around 24 + 2 + 2 = 28e-. If we look at the ELF populations for the neutral system, we appreciate that both iron cores are very similar, although one of them is slightly less populated. Instead, the Fe-C basins present subtle differences between them, depending on their relative positions with respect to the thiol chain.

After the first oxidation, the cation presents the Fe(1) core with an almost negligible variation of +0.01e-, whereas the Fe(2) core is most affected by -0.15e-. However, the Fe-C basins are very different: the Fe(1)-C cores vary -0.16e- whereas the Fe(2)-C cores vary -0.73e-. In other words, Fe(1) and its surroundings lose -0.15e- in total, in contrast to the -0.88e- of Fe(2) and its surroundings. This means a very small density gaining in the rest of the system (+0.03e-) to account for the one electron lost in the process. This would mean that the ferrocenyl unit attached to CSR is the one that assumes most of the oxidation.

It is worth mentioning that the cationic structure is an equilibrium structure obtained after relaxing the whole structure, i.e., we extract the electron and let the system to reorganize its electron density. The experimental results are not obtained in equilibrium conditions. Moreover, the calculations are carried out for pure isomers in vacuum, whereas the experiment in solution might present a certain mixture.

A similar analysis carried out with the populations extracted from the NBO method, although offering a different partition of the system, is in line with the results shown by the ELF.